Journal of Power Sources 196 (2011) 2241–2245

Contents lists available at ScienceDirect

Journal of Power Sources

journal homepage: www.elsevier.com/locate/jpowsour

Short communication

Preparation and electrochemical investigation of Li_2CoPO_4F cathode material for lithium-ion batteries

Deyu Wang[a], Jie Xiao[a], Wu Xu[a], Zimin Nie[a], Chongmin Wang[b], Gordon Graff[a], Ji-Guang Zhang[a,*]

[a] Energy and Environment Directorate, Pacific Northwest National Laboratory, Richland, WA 99354, USA
[b] Environmental Molecular Sciences Laboratory, Pacific Northwest National Laboratory, Richland, WA 99354, USA

ARTICLE INFO

Article history:
Received 23 August 2010
Received in revised form 5 October 2010
Accepted 5 October 2010
Available online 13 October 2010

Keywords:
Li_2CoPO_4F
Fluorophosphate
High-voltage cathode
Lithium-ion battery
Cathode
Electrolyte

ABSTRACT

In this paper, we report the electrochemical characteristics of a novel cathode material, Li_2CoPO_4F, prepared by solid-state reactions. The solid-state reaction mechanism involved in synthesizing the Li_2CoPO_4F also is analyzed in this paper. When cycled between 2.0 V and 5.0 V during cyclic voltammetry measurements, the Li_2CoPO_4F samples present one, fully reversible anodic reaction at 4.81 V. When cycled between 2.0 V and 5.5 V, peaks occurring at 4.81 V and 5.12 V in the first anodic scan evolved to one broad oxidative, mound-like pattern in subsequent cycles. Correspondingly, the X-ray diffraction (XRD) pattern of the Li_2CoPO_4F electrode discharged from 5.5 V to 2.0 V is slightly different from the patterns exhibited by a fresh sample and the sample discharged from 5.0 V to 2.0 V. This difference may correspond to a structural relaxation that appears above 5 V. In the constant current cycling measurements, the Li_2CoPO_4F samples exhibited a capacity as high as 109 mAh g^{-1} and maintained a good cyclability between 2.0 V and 5.5 V vs. Li/Li^+. XRD measurements confirmed that the discharged state is Li_2CoPO_4F. Combining these XRD results and electrochemical data proved that up to 1 mol Li^+ is extractable when charged to 5.5 V.

Published by Elsevier B.V.

1. Introduction

Since the first commercialization of lithium-ion batteries in the 1990s, novel electrode materials have been intensely pursued by the researchers worldwide to meet the ever-increasing demand for high-energy-density batteries. Recently, Li_2MPO_4F materials (M = Fe, Co, Mn) have been proposed as promising candidates for high-energy-cathode materials [1–5]. These materials could be considered to incorporate LiF into the lattice structure of phosphor comparatives. This incorporation reaction changes the crystal symmetry of the original phosphor-olivines and results in a three-dimensional framework composed of PO_4 and MO_4F_2 [2]. In addition to the expected thermal stability, which is similar to olivine phosphate, the potential incorporation of a second Li^+ ion in Li_2MPO_4F (M = Fe, Co, Mn) may lead to a specific capacity as high as *ca.* 290 mAh g^{-1}. The structural and electrochemical characteristics of Li_2/Na_2FePO_4F have been investigated by Nazar's group [1–3]. Despite unsuccessful attempts to extract the second Li^+ ion electrochemically, realizing a high-capacity cathode still appears to be possible because both Na^+ ions in Na_2FePO_4F have been chemically displaced [1].

Li_2CoPO_4F is another promising candidate in this family of materials. Because of the higher ionicity of M–F bonds, the working plateau of Li_2CoPO_4F should be higher than that of $LiCoPO_4$ (4.8 V vs. Li/Li^+). In other words, Li_2CoPO_4F possesses the highest redox potential among currently available cathodes, which makes it an attractive candidate material for cathodes used in high-energy batteries. The preparation and structural analysis of this material has been reported by Okada et al. [6]. However, to date, very limited electrochemical characteristics of Li_2CoPO_4F have been reported. Recently, Khasanova et al. [7] reported on the electrochemical performance of Li_2CoPO_4F in a conventional electrolyte based on carbonate solvents. However, the electrochemical characteristics of Li_2CoPO_4F reported by Nellie et al. are unclear because of the limited electrochemical window of the electrolyte used in their experiments.

In this paper, we report the synthesis and electrochemical performance of the novel cathode Li_2CoPO_4F. In contrast the micro-level particles studied by Okada et al. [6], the samples prepared using our modified calcination process exhibit typical particle sizes ranging from 300 nm to 500 nm. The prepared Li_2CoPO_4F/C is evaluated with a sulfone-based electrolyte, which is stable up to 5.5 V vs. Li/Li^+ [8,9]. The correlations between the electrochemical performances and structure changes in this material also are discussed.

2. Experimental

For our experiments, Li_2CoPO_4F was prepared using solid-state reactions using lithium fluoride as the only lithium precursor [10]. A mixture of $Co(CH_3COO)_2{\cdot}4H_2O$ (Aldrich, 99.9%), $NH_4H_2PO_4$

* Corresponding author. Tel.: +1 509 372 6515; fax: +1 509 375 3864.
E-mail address: jiguang.zhang@pnl.gov (J.-G. Zhang).

0378-7753/$ – see front matter. Published by Elsevier B.V.
doi:10.1016/j.jpowsour.2010.10.021

(Aldrich, 99%), and LiF (Aldrich, 99%) in a molar ratio of 1:1:2, respectively, was mixed and ground with Super P carbon (5 wt% of Li_2CoPO_4F, Timical) and 2-isopropanol (300 ml mol^{-1} of Li_2CoPO_4F) in a ball mill (Spex 8000) for 3 h. The milled mixture was sintered in a tube furnace under an Ar–H_2 (97.4:2.6, v/v) flow at 400 °C for 8 h. After re-milling for another 30 min, the mixture was further sintered at 600 °C for 24 h and then 700 °C for another 24 h.

The electrolyte used in this work is 1 mol $LiPF_6$ in a mixture of dimethyl sulfone (DMS) and ethyl methyl sulfone (EMS) (85:15, w/w). This electrolyte is reported to be stable up to 5.5 V vs. Li/Li^+ [8,9]. The DMS (powder, 98%, Aldrich) and EMS (powder, 98%, TCI) first were sublimed to eliminate absorbed moisture, and then transferred to a glove box for storage. The EMS, DMS, and $LiPF_6$ constituents were placed in a glass vial at a weight ratio of 74.74:13.21:12.05, respectively. The mixture was fully liquidized after a few hours.

The electrode was prepared by casting the slurries containing 70 wt% Li_2CoPO_4F/C, 15 wt% Super P, and 15 wt% poly(vinylidene fluoride) (PVdF) (HSV 900, Kynar) in *N*-methyl-pyrollidone on a 25-μm-thick aluminum foil (UHV foil, Texas Technology). To investigate the source of low columbic efficiency in the samples, electrodes with no active material (Super P: PVdF = 8:2, w/w) also were prepared using a similar approach. After drying at 100 °C under vacuum overnight and pressing under 65 MPa, the electrode was punched into ϕ 1.4-cm disks with an average loading of 2 mg active material. The thickness of the film is ~30 μm. The electrode disks subsequently were assembled into Type 2325 coin cells (NRC, Canada) composed of a Li-metal-foil anode, a glass-fiber separator (GF/D, Whatman), and the previously identified electrolyte. The test cells were assembled in an MBraun glove box filled with purified argon.

The cells with Li_2CoPO_4F cathode were cycled between 2.0 V and 5.0 V or 2.0 V and 5.5 V ranges on an Arbin BT 2000 battery tester at a constant current of 10 μA. The capacity was calculated based on the amount of active materials in the cells. The electrodes subjected to different charge/discharge states were recovered by disassembling the corresponding cells in a fume hood. After washing three times with dimethyl carbonate and drying overnight in a vacuum oven at room temperature, the electrodes were stored in a sealed bottle for *ex situ* XRD measurements.

Cyclic voltammetry (CV) tests were conducted on a PC-controlled CH Instrument 660C Potentiostat/Galvanostat between 2.5 V and 5.0 V or 2.5 V and 5.5 V ranges at a 0.1 mV s^{-1} scan rate. Powder XRD measurements were performed using a Philips Xpert X-ray diffractometer in $\theta - 2\theta$ scan mode and a CuKα sealed tube

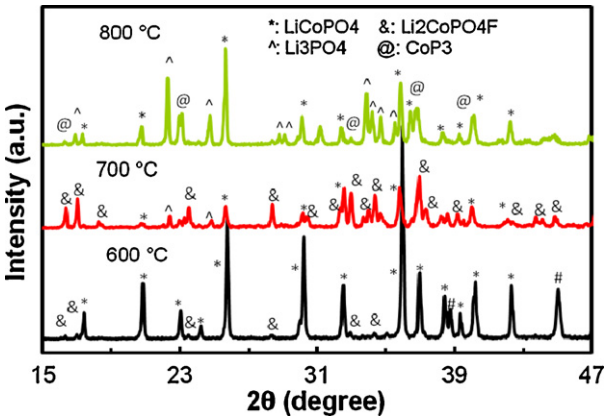

Fig. 1. Powder XRD patterns of samples prepared at 600 °C, 700 °C, and 800 °C.

(λ = 1.54178 Å) at 0.5 ° min^{-1}. High-resolution transmission electron microscopy (TEM) analysis was carried out on a Jeol JEM 2010 microscope fitted with a LaB_6 filament and an acceleration voltage of 200 kV.

3. Results and discussion

Fig. 1 shows the XRD pattern of the samples prepared at different temperatures. For the material synthesized at 600 °C, $LiCoPO_4$ is the dominant phase, and LiF also is present. A trace amount of Li_2CoPO_4F is formed at this temperature. When the sintering temperature is increased to 700 °C, Li_2CoPO_4F becomes the dominate phase, and $LiCoPO_4$ and Li_3PO_4 also are present. At 800 °C, the sample does not contain Li_2CoPO_4F. Instead, it is composed of CoP_3, $LiCoPO_4$, and Li_3PO_4. These experimental results clearly elucidate the following reaction mechanism: (1) $LiCoPO_4$ can be obtained at 600 °C (Eq. (1)); (2) Li_2CoPO_4F begins to form at 600 °C in a very low rate and becomes dominant at 700 °C (Eq. (2)); and (3) the side reaction to produce Li_3PO_4 takes place at a temperature higher than 600 °C (Eq. (3)) [10].

$$\text{Reaction}: \text{CoO} + \text{DP} + \text{LiF} \rightarrow \text{LiCoPO}_4 \quad \geq 600\,^{\circ}\text{C} \tag{1}$$

$$\text{LiCoPO}_4 + \text{LiF} \rightarrow \text{Li}_2\text{CoPO}_4\text{F} \quad \geq 700\,^{\circ}\text{C} \tag{2}$$

$$\text{Sidereaction}: \text{LiF} + \text{DP} \rightarrow \text{Li}_3\text{PO}_4 \quad > 600\,^{\circ}\text{C} \tag{3}$$

where DP represents the decomposed product of $NH_4H_2PO_4$. To obtain pure-phase Li_2CoPO_4F, a sample was calcined at 600 °C for 24 h to form $LiCoPO_4$, and then at 700 °C for 24 h to produce

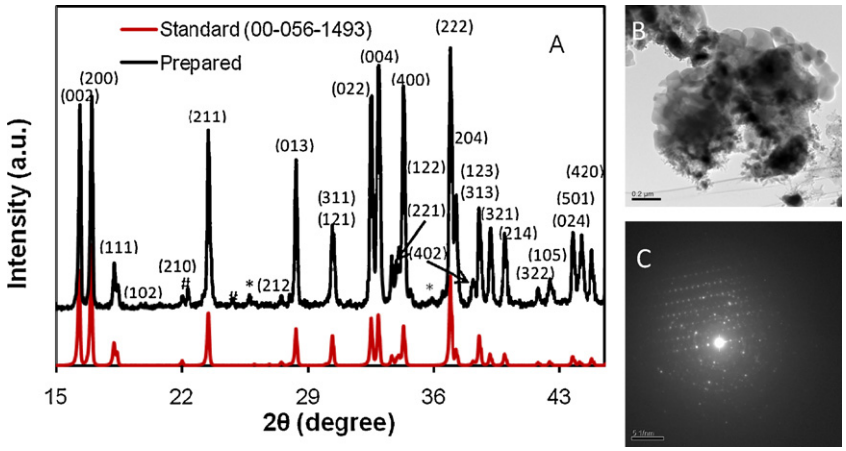

Fig. 2. Powder XRD patterns (A) and corresponding TEM micrographs (B, C) of the prepared Li_2CoPO_4F sample. The XRD peaks corresponding to Li_3PO_4 and $LiCoPO_4$ are represented by the symbols # and *, respectively.

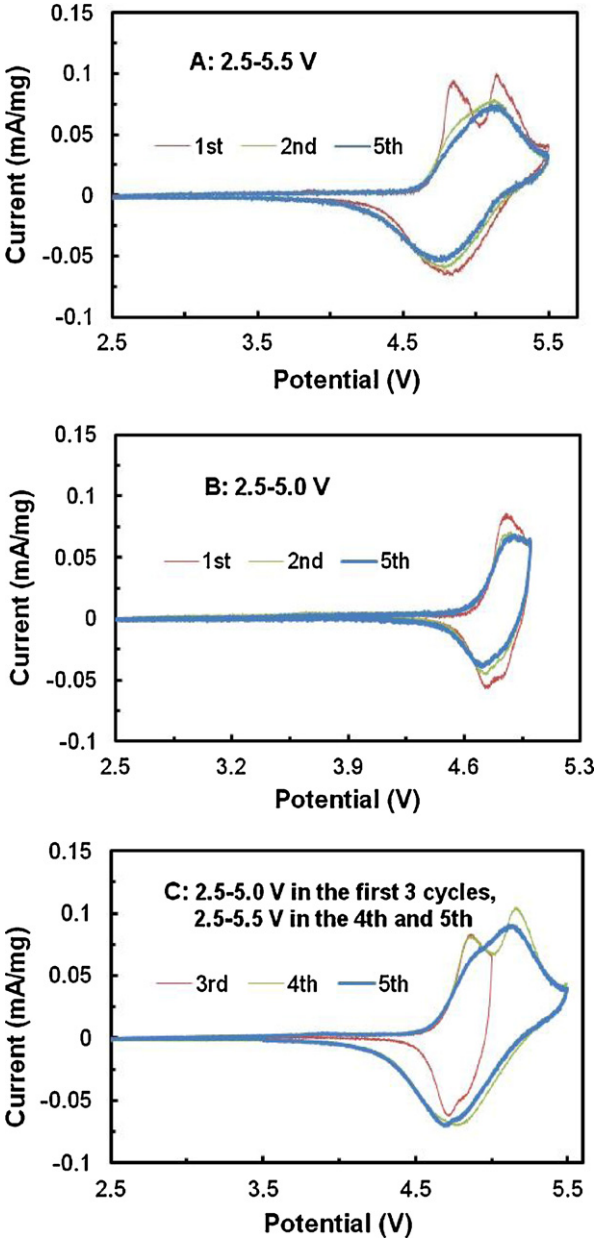

Fig. 3. CV curves of Li_2CoPO_4F with different scanned ranges. The scanning rate was 0.1 mV s^{-1}.

Li_2CoPO_4F. As indicated by the XRD data, the material obtained is almost pure-phase Li_2CoPO_4F with trace amounts of $LiCoPO_4$ and Li_3PO_4 (Fig. 2A). Li_2CoPO_4F is indexed in the *Pnma* space group of the orthorhombic system, with a lattice parameter of $a = 10.454(6)$ Å, $b = 6.381(4)$ Å, $c = 10.862(2)$ Å, and $V = 724.60$ Å^3. The particle size is *ca.* 300–500 nm based on TEM imaging as shown in Fig. 2B. Although some impurities exist in this sample, they do not significantly affect its electrochemical behavior.

The CV curves of the Li_2CoPO_4F samples are compared in Fig. 3. When the sample was scanned between 2.5 V and 5.5 V, as shown in Fig. 3A, two sharp oxidative peaks, located at 4.81 V and 5.12 V, in the first anodic scan evolve to one broad oxidative, mound-like pattern in the subsequent cycles. The capacities in the first two anodic scans are 153 mAh g^{-1} and 137 mAh g^{-1}, respectively, and 72 mAh g^{-1} and 80 mAh g^{-1} for the corresponding cathodic scans. This observation probably indicates that the second Li^+ ion actually is not extractable up to 5.5 V. The low columbic efficiency may result from electrolyte decomposition on the conductive carbon and the active material, which will be discussed in the later part of this article.

The shape change in the curves of the initial cycles indicates that an irreversible relaxation occurs in the microstructure of the Li_2CoPO_4F. The presence of two oxidative peaks in the first anodic scan implies that Li^+ ions are extracted from the two energetically inequivalent crystallographic sites in the Li_2CoPO_4F's framework. The merging of the two peaks in the subsequent scans indicates that the difference between the two inequivalent sites is eliminated by a structural relaxation occurring during the first charging process.

Fig. 3B shows the CV curves of the cell cycled between 2.5 V and 5.0 V, with the purpose of determining the reaction that occurs at 4.81 V. The CV curves show charge/discharge capacities of *ca.* 70 mAh g^{-1} and 40 mAh g^{-1}, respectively, which are about half the values of cells scanned to 5.5 V. These results demonstrate that this reaction is iso-electronic with the reaction occurring above 5.0 V. In addition, the CV curves maintain a similar shape, although the peak values are slightly lower in the subsequent cycles. This result indicates that this reaction does not lead to the aforementioned structural relaxation. To validate this assumption, a cell was tested between 2.5 V and 5.0 V in the first three cycles, and then scanned between 2.5 V and 5.5 V for another two cycles. As shown in Fig. 3C, two oxidative peaks still appear in the fourth cycle. This finding confirms that elimination of the energetically inequivalent sites in the Li_2CoPO_4F framework is associated only with the reaction occurring at the higher potential.

Fig. 4 depicts the charge–discharge curves of Li_2CoPO_4F. When cycled between 5.5 V and 2.0 V vs. Li/Li^+, Li_2CoPO_4F delivers a reversible capacity of *ca.*109 mAh g^{-1}, which is twice the capacity of the cells cycled between 2.0 and 5.0 V vs. Li/Li^+. The inset in Fig. 4A represents the initial part of discharge profiles, which clearly illustrates that Li_2CoPO_4F begins to discharge at ~5.1 V vs. Li/Li^+. These results agree well with the observations from the CV measurements. Similar to Li_2FePO_4F, the discharge curve of Li_2CoPO_4F exhibits a slope rather than a flat plateau, probably indicating that its charge–discharge mechanism is different from that of olivine materials. As shown in Fig. 4B, no obvious capacity fading was observed within 20 cycles for both measurements. However, the low columbic efficiency, which probably is caused by electrolyte decomposition at high voltages, is noticed as shown in Fig. 4B. As a control sample, carbon/lithium cells were tested between 2.0 V and 5.5 V using the same electrolyte. As shown in Fig. 4C, the charge capacity at the first cycle reaches 540 mAh g^{-1}, a large portion of which is irreversible and corresponds to the electrolyte decomposing on the surface of the Super P carbon at high voltage. The irreversible capacity diminished rapidly in subsequent cycles, and stabilized at ~50 mAh g^{-1} after the fifth cycle. The total irreversible capacity of the test cells including the contributions from the carbon additive (SP) and the active material and can be represented by Eq. (4):

$$Cap_{ir\text{-}total} = Cap_{ir\text{-}SP} + Cap_{ir\text{-}LCPF} \quad (4)$$

where $Cap_{ir\text{-}SP}$ is calculated from a Super P control cell, $Cap_{ir\text{-}LCPF}$ is the difference between $Cap_{ir\text{-}total}$ and $Cap_{ir\text{-}SP}$. The data shown in Fig. 4D was plotted from Eq. (4) to explore the origin of the low columbic efficiency. To compare the practical irreversible capacities from individual component in the cells, the units of the Y-axis in Fig. 4D is mAh rather than mAh g^{-1}. As shown in Fig. 4D, the large irreversible capacity in the first two cycles is mainly from the electrolyte decomposition on the Super P carbon. The side reaction between the Li_2CoPO_4F and the electrolyte is the key reason for the low efficiency in the subsequent cycles. We also observed that the irreversible capacity is still significant after the tenth cycle. This observation indicates that the solvents continue to decompose on the surfaces of the carbon and the active material, although the state-of-art 5-V electrolyte was used in these experiments. To fur-

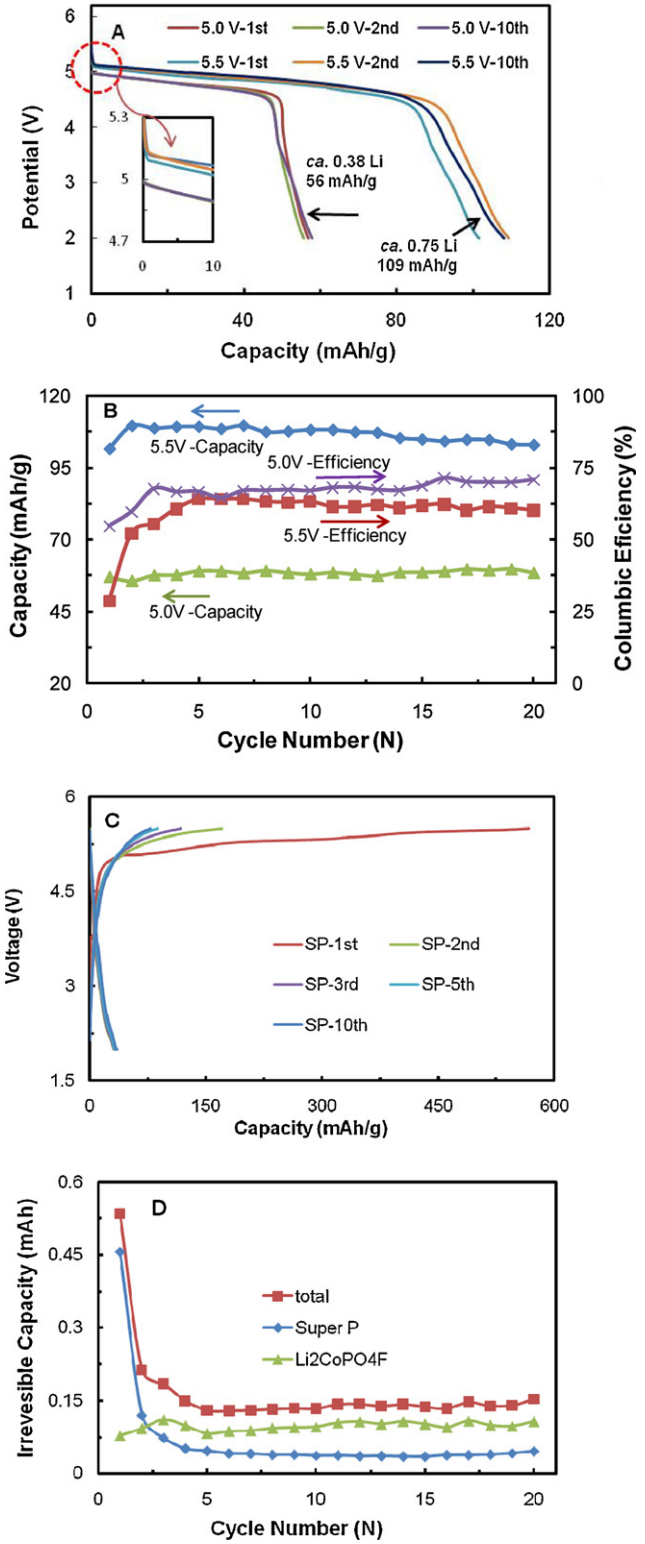

Fig. 4. Charge/discharge performances of Li_2CoPO_4F cathodes cycled between 2.0 V and 5.0 V or 2.0 V and 5.5 V. The cells were tested with a constant current of 10 μA. (A) Discharge curves; (B) cycling performance; (C) charge–discharge curves of Super P electrode; (D) irreversible capacity analysis. Irreversible capacity of Super P: calculated from control electrode; irreversible capacity of Li_2CoPO_4F: the difference between from the total and super P part.

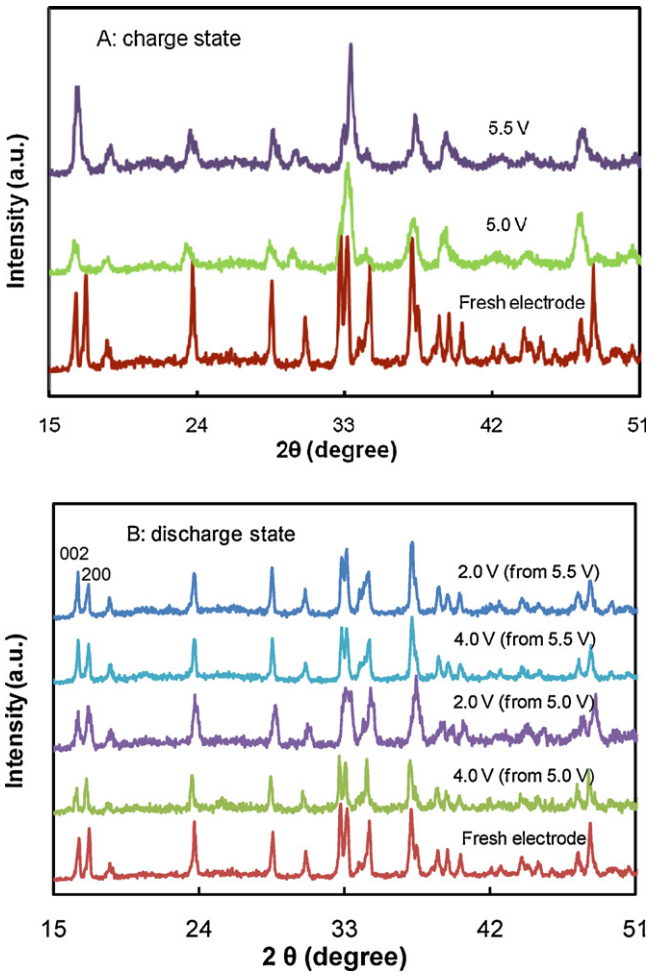

Fig. 5. XRD patterns of Li_2CoPO_4F electrodes at different stages of cycling during the first charge–discharge cycle.

ther improve the stability of the cathode, an electrolyte that can form a stable solid electrolyte interface on the cathode surface is required.

To trace the structural evolvement during cycling, we compared the XRD patterns of electrodes at different potentials in the first cycle. As shown in Fig. 5A, a clear structural change is observed after the material charged to 5.0 V and 5.5 V vs. Li/Li^+. Li_2CoPO_4F is not detected inside both electrodes, confirming that its reaction mechanism different from olivine phosphates. The structural variations during the charge/discharge processes will be investigated further using *in situ* X-ray measurements. Fig. 4B shows that the electrodes discharged to 4.0 V and 2.0 V exhibit XRD patterns that are similar to the patterns exhibited by fresh samples before charging. This observation indicates that the extracted Li^+ ions are almost fully reinserted into the original cathode structure. Combining this result and capacity data proves that this is a one-electron reaction up to 5.5 V. Upon closer comparison, the XRD patterns of the electrodes discharged from 5.5 V exhibit some minor changes from those of the others. For example, the (0 0 2) peak is stronger than the (2 0 0) peak for the electrodes discharged from 5.5 V; whereas, the XRD patterns of electrodes discharged from 5.0 V maintain the same trend as the fresh electrodes. This difference indicates that the structural relaxation of the framework of Li_2CoPO_4F occurs at a voltage greater than 5.0 V, which is consistent with the CV measurements.

Although only one Li^+ ion can be reversibly cycled as reported in this work, Li_2CoPO_4F is still a promising cathode material. It could be a competitive candidate for the cathode of a high-energy bat-

tery because of its theoretical capacity of 143 mAh g^{-1} and the high discharge voltage between 5.1 V and ~4.6 V. It is also more stable at high voltage when compared with most of other cathodes based on lithium metal oxide [6]. With the development of a more stable electrolyte and compatible conductive additive, it is also possible that the second lithium in Li_2CoPO_4F can be extracted and the capacity of the cathode can be further increased. More accurate theoretical simulations will be needed to provide accurate predictions of the redox potential, and the stability of Li_2CoPO_4F at high potentials.

4. Conclusions

We successfully prepared Li_2CoPO_4F, and investigated its electrochemical performance using a high-voltage electrolyte. When charged to 5.5 V, one Li^+ ion could be extracted from the framework of the Li_2CoPO_4F. This observation probably indicates that a much higher energetic barrier needs to be overcome to extract the second Li^+ ion. Despite the 109 mAh g^{-1} capacity attained in our work, a higher capacity is predicted for Li_2CoPO_4F after adopting appropriate strategies based on the successful experience with $LiFePO_4$ and $LiMnPO_4$. The stability of this material also is good at high potentials, at least to 5.5 V, although the solvents continuing to decompose on the surface of active material and carbon resulted in the low coulomb efficiency of the samples. Therefore the full potential of the Li_2CoPO_4F cathode will be determined when a better-matched electrolyte and suitable conductive additive are developed.

Acknowledgement

The authors are grateful for financial support from the Laboratory Directed Research and Development Program at Pacific Northwest National Laboratory (PNNL) and the Batteries for Advanced Transportation Technologies (BATT) program at the Office of Vehicle Technologies of the U.S. Department of Energy (DOE). The TEM work was performed in the Environmental Molecular Sciences Laboratory, a national scientific user facility sponsored by DOE's Office of Biological and Environmental Research and located at PNNL.

References

[1] B.L. Ellis, W.R.M. Makahnouk, Y. Makimura, K. Toghill, L.F. Nazar, Nature Mater. 6 (2007) 749.
[2] B.L. Ellis, W.R.M. Makahnouk, W.N. Rowan-Weetaluktuk, D.H. Ryan, L.F. Nazar, Chem. Mater. 22 (2010) 1059.
[3] T.N. Ramesh, K.T. Lee, B.L. Ellis, L.F. Nazar, Electrochem. Solid State Lett. 13 (2010) A43.
[4] M.E.A. Dompablo, U. Amador, J.-M. Tarascon, J. Power Sources 174 (2007) 1251.
[5] M. Ramzan, S. Lebegue, P. Larsson, R. Ahujia, J. Appl. Phys. 106 (2009) 043510.
[6] S. Okada, M. Ueno, Y. Uebou, J. Yamaki, J. Power Sources 146 (2005) 565.
[7] N.R. Khasanova, A.N. Gavrilov, E.V. Antipov, K.G. Bramnik, H. Hibst, J. Power Sources (in press).
[8] K. Xu, C.A. Angell, J. Electrochem. Soc. 149 (1998) L70.
[9] A. Abouimrane, I. Belharouak, K. Amine, Electrochem. Commun. 11 (2009) 1073.
[10] D. Wang, H. Li, Z. Wang, X. Wu, Y. Sun, X. Huang, L. Chen, J. Solid State Chem. 177 (2004) 4582.